Available online at www.sciencedirect.com

SciVerse ScienceDirect

Ceramics International 39 (2013) 6853–6859

CERAMICS INTERNATIONAL

www.elsevier.com/locate/ceramint

Preparation and characterization of AlN/FeCoSiB magnetoelectric thin film composites

Bei Tong, Xiaofei Yang, Zhe Guo, Kun Li, Jun Ouyang, Gengqi Lin, Shi Chen*

School of Optical and Electronic Information, Huazhong University of Science and Technology, Wuhan, Hubei 430074, China

Received 17 January 2013; received in revised form 4 February 2013; accepted 5 February 2013
Available online 17 February 2013

Abstract

The preparation process of AlN/FeCoSiB thin film composites has been studied in detail in this work. The results indicate that annealing is more effective to improve the intensity of AlN (002) peak compared with changing sputtering parameters. After annealing at 500 °C, the AlN film possesses the highest intensity of (002) peak, typical columnar microstructure and root-mean-square (rms) roughness of 5 nm. The coercivity (H_c) of FeCoSiB film decreases significantly after annealing in magnetic field. After annealing at 350 °C, a minimum H_c of 2.6 Oe is obtained in FeCoSiB film, contributing to the achievement of most pronounced magnetic field sensitivity. The magnetoelectric (ME) voltage coefficient α_{ME} up to 101 V/cm Oe is obtained at DC bias magnetic field (H_{dc}) of 10 Oe and at the frequency (f) of 1 kHz. Furthermore, the thin film composites display an AC magnetic field sensitivity of 1.6 nT/$\sqrt{}$Hz at 1 kHz.

Keywords: AlN/FeCoSiB; Preparation; Magnetoelectric; Thin film; Sensitivity

1. Introduction

It is well- known that in comparison with single-phase magnetoelectric (ME) materials [1,2], the ME composites [3–5] which consist of piezoelectric and magnetostrictive materials have attracted great attention in the past few years owing to their higher ME coefficient and maximum operation temperature [6]. In such composites, the ME effect is a result of the product of the magnetostrictive effect (magnetic/mechanical effect) in the magnetic phase and the piezoelectric effect (mechanical/electrical effect) in the piezoelectric one [7]. Although they exhibit interesting characteristics, most of these composites are still bulk materials and therefore hard to integrate in Micro-Electro-Mechanical-Systems (MEMS) or microelectronic devices [8]. In recent years, ME thin film composites have aroused considerable interest due to many unique superiorities compared with bulk or laminated ME composites. For instance, ME thin film composites are more reliable than gluing laminated devices with epoxy resin because the ME coupling is achieved through natural adhesion of one thin film deposited on another. In addition, the different phases could be combined and designed at atomic-level by precisely controlling the lattice matching. From the application viewpoint, ME thin film composites are promising candidates in integrated magnetic/electric devices, such as ME random access memories [9] ME microsensor [10] and so on. However, it is particularly important that the preparation of ME thin film composites with high quality should be highly desired to achieve these superiorities, which can be accomplished by utilizing a wide variety of growth techniques such as PLD, MBE, sputtering, spin coating, MOCVD, and more. In general, the PLD [11–15] and sol–gel spin coating [16–19] are practiced widely in the research of oxide ME thin film preparation, while the non-oxide ME thin film is deposited mainly by RF magnetron sputtering. Recently, the giant ME effect of AlN/FeCoSiB thin film composites fabricated by RF magnetron sputtering has been reported to possess the highest ME coefficients in thin film composites by now [20–22]. Such a high ME response is closely related to respective properties of piezoelectric layer and magnetostrictive layer. However, few papers have been published dealing with the preparation process of AlN/FeCoSiB thin film composites. Therefore, the detailed

*Corresponding author. Tel.: +86 27 87542893; fax: +86 27 87558209.
E-mail address: s_chen@sina.com (S. Chen).

0272-8842/$ - see front matter © 2013 Elsevier Ltd and Techna Group S.r.l. All rights reserved.
http://dx.doi.org/10.1016/j.ceramint.2013.02.019

preparation process of AlN/FeCoSiB ME thin film composites is investigated in this paper which contains several parts as follows. Firstly, the orientation, microstructure and surface roughness of AlN film at different sputtering parameters and annealing conditions are studied in detail. Based on the first part, the second is to investigate the deposition process of FeCoSiB film on Si/SiO_2/AlN substrate and the effect of magnetic field annealing on magnetic properties of FeCoSiB film. Lastly, the ME voltage coefficient α_{ME} of the AlN/FeCoSiB thin film composites as a function of DC bias magnetic field (H_{dc}) and AC magnet field (H_{ac}) at low frequency ($f=1$ kHz) is evaluated.

2. Experimental procedures

To fabricate such AlN/FeCoSiB ME thin film composites with longitudinal magnetization–transverse polarization (*L–T*) working mode, the target of molybdenum (Mo), aluminum (Al), FeCoSiB and the Si/SiO_2 substrates were used as the starting materials. Firstly, a 300 nm Mo film used as the bottom electrode was deposited on the Si/SiO_2 substrate by RF magnetron sputtering (SPF-430H, ANELVA, Japan). Secondly, the piezoelectric AlN layer with thickness of 1.2 μm was deposited by reactive magnetron sputtering. Lastly, the magnetostrictive layer, 1.5 μm thick FeCoSiB which simultaneously acts as the top electrode was deposited on AlN film. The thin film composites were bonded to PCB board with epoxy resin and the electrodes were welded by aluminum wire bonder (Fig. 1). Applying H_{dc} and H_{ac} to the long axis of the cantilever will lead to a ME voltage U_{ME} between the Mo layer and the FeCoSiB magnetostrictive layer.

The crystal structure of the AlN film and its orientation were analyzed by X-ray diffraction (XRD, X' Pert PRO, PANalytical). The cross-sectional microstructure of the AlN film and the interface between AlN and FeCoSiB layers were observed using a Field Emission Scanning Electron Microscope (FESEM, FEI Quanta 450FEG). Furthermore, Atomic Force Microscope (AFM, Veeco Nanoscope's Contact Mode) was utilized to facilitate a detailed analysis of the surface morphology and surface roughness of AlN film. The AFM analysis was carried out in contact mode using a scan size area of 2 μm^2. The magnetic measurements were performed with vibrating sample magnetometer (VSM, Lake Shore, 7400) and the ultra-depth 3D microscope (VHX-1000E) was used for morphology observation of FeCoSiB film. The H_{ac} was generated through a long straight solenoid with 200-turn coils driven by a single generator. The H_{dc} was supplied by a pair of NbFeB permanent magnets. The output *p–p* voltage signal generated from the piezoelectric AlN film induced by the in-plane magnetic field was provided to Charge Amplifier and then detected using Spectrum Analyzer (Agilent, 35670A). All the measurements above were carried out at room temperature. The prepared AlN/FeCoSiB thin film composites and measurement setup for ME voltage were shown in Fig. 2.

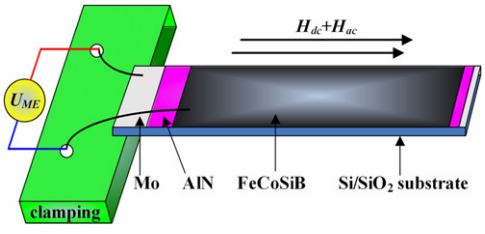

Fig. 1. Schematic illustration of the fabricated structure.

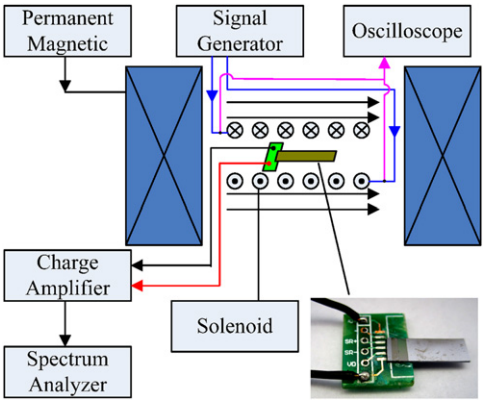

Fig. 2. Schematic of AlN/FeCoSiB sample and ME measurement setup.

3. Results and discussion

3.1. Preparation and structure of AlN film

For the fabrication of AlN/FeCoSiB ME thin film composites, the key is to obtain (002) texture (*c*-axis oriented) AlN film on Si/SiO_2/Mo substrates. Before the deposition of AlN film, a Mo under-layer was deposited on the Si/SiO_2 substrate as a bottom electrode with deposition pressure of 4 mTorr, substrate to target distance of 8 cm and sputtering power of 300 W. The deposition process lasted for 12 min without heating the substrate. Many attempts by changing the sputtering conditions such as substrate temperature, gas flow ratio of Ar and N_2, sputtering power and so on have been tried to grow (002) preferred oriented AlN film successfully. Therefore, in this work, for purpose of validation, the influence of deposition conditions such as substrate to target distance, sputtering gas and pressure, substrate temperature and RF power on AlN texture is studied in detail. Table 1 summarizes the deposition parameters for five groups of samples. The XRD patterns of corresponding AlN film prepared according to Table 1 are shown in Fig. 3. The results are concluded as follows: (1) reducing the distance of substrate to target can inhibit the formation of (100) texture of AlN; (2) increasing the volume fraction of N_2 can promote formation of AlN (002) texture; (3) substrate heating is not conducive for the formation of (002) peak but lead to emergence of (100) peak; (4) high sputtering power is beneficial for growth of AlN with an (002) orientation, which is consistent to the previous results [23–25]. Based on the results above, the deposition parameters of 3#AlN is chosen as the best solution.

Table 1
Deposition parameters for AlN film.

Parameters[a]	1#	2#	3#	4#	5#
Substrate to target distance(mm)	50	40	40	40	40
Sputtering gas and pressure(mTorr)	$1Ar+2N_2$	$1Ar+2N_2$	$1Ar+3N_2$	$1Ar+3N_2$	$1Ar+3N_2$
Substrate temperature(°C)	Unheated	Unheated	Unheated	250	250
RF power(W)	400	400	400	400	600

[a]Other deposition parameters are: Al target with purity 99.999%, base pressure $<7.5\times10^{-4}$ Pa and sputtering time is 40 min.

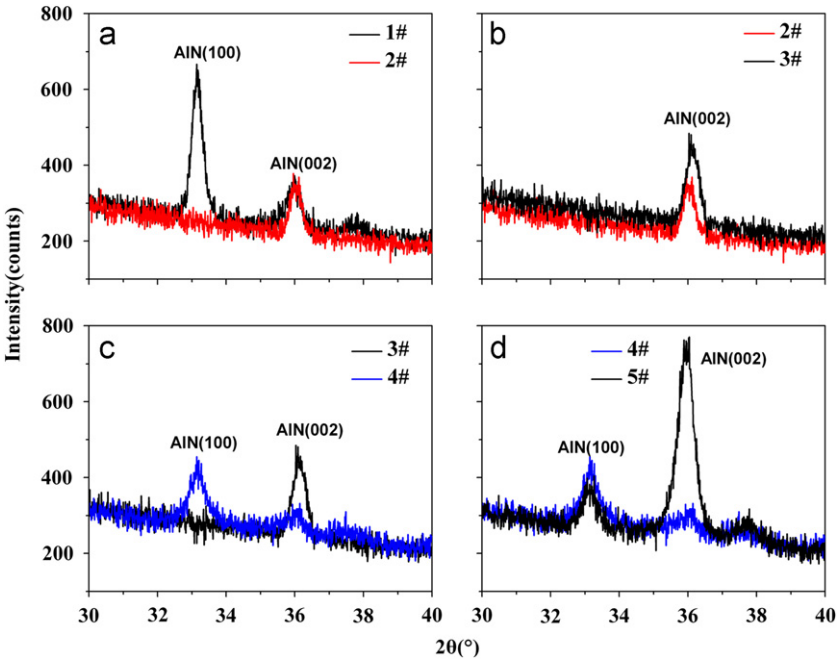

Fig. 3. XRD patterns of AlN film at different conditions including (a) substrate to target distance; (b) sputtering gas and pressure; (c) substrate temperature; (d) sputtering power.

However, it can be seen from Fig. 3 that only changing the sputtering parameters is not a good way to improve the intensity of AlN (002) peak. Therefore, the effect of annealing temperature on texture and microstructure of AlN film was studied in detail to investigate the feasibility of obtaining the (002) AlN texture. After being deposited on Mo bottom electrode, the AlN film according to deposition parameters of 3# AlN sample was heat-treated at different annealing temperatures of 400 °C, 500 °C and 600 °C for 30 min in a vacuum of 5.0×10^{-4} Pa.

The XRD patterns of corresponding AlN film annealed at different temperatures are shown in Fig. 4. It is apparent that each AlN film shows a main diffraction peak near $2\theta=36.1^\circ$ which corresponds to the AlN (002) crystal orientation. Meanwhile, the intensity of (002) crystal orientation increases significantly after heat-treating, which can be attributed to (1) the relieving of internal stress and (2) further growth of grain through the effective heat-treatment process. Furthermore, it also can be observed that the diffraction intensity of (002) peak increases firstly and reduces afterward with increasing the annealing temperature. Among them, 500 °C is the most suitable annealing temperature to obtain the strongest diffraction intensity of (002) peak which indicates the largest piezoelectric coefficient of AlN film.

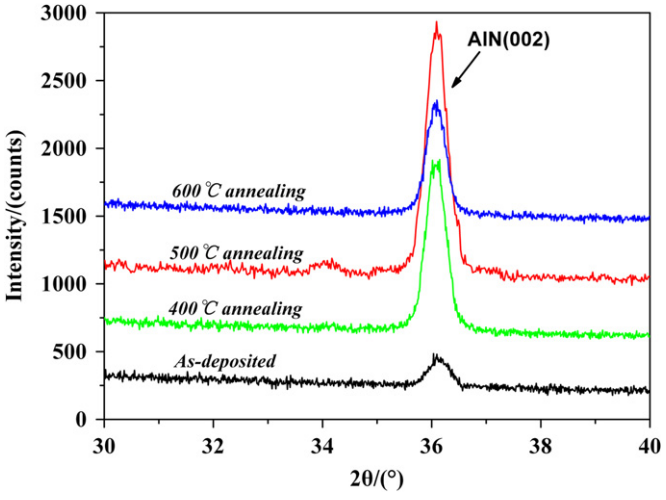

Fig. 4. XRD patterns of AlN film at different annealing temperatures.

Fig. 5 presents FESEM micrograph of the cross-sectional microstructure of AlN film annealed at 500 °C. It can be seen that the AlN film exhibits a typical dense

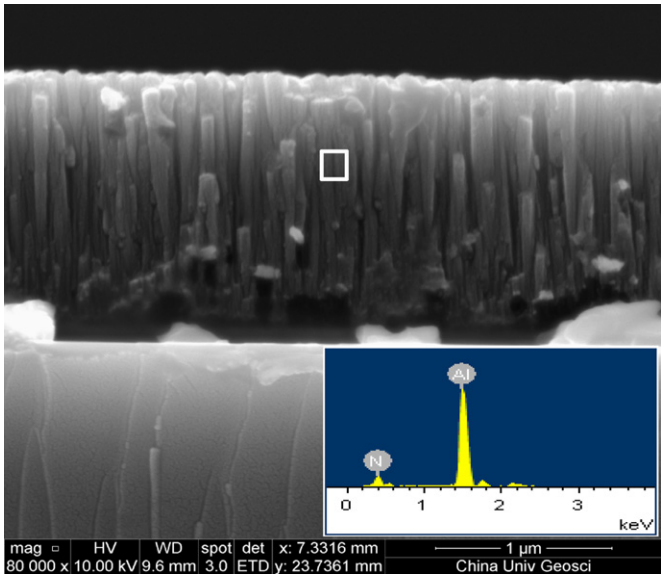

Fig. 5. Cross-sectional SEM of AlN film at annealing temperature of 500 °C.

and (002) oriented columnar structure. Moreover, the EDX area analysis indicates this columnar contains only Al and N elements (i.e., AlN), which is in accordance with XRD analysis.

In order to further observe the surface roughness of AlN film, a statistical analysis of AlN film as-deposited and annealed at 500 °C is carried out by means of AFM technique, as can be seen in Fig. 6. The rms roughness of the as-deposited AlN film is 9.8 nm (Fig. 6(a)) while it is 5 nm for the AlN film annealed at 500 °C (Fig. 6(b)) which decreased by nearly 50% compared to the former one. That is to say, the AlN film annealed at 500 °C has a smoother upper surface.

3.2. Preparation of FeCoSiB film

Based on the results above, it is confirmed that the AlN film possesses high *c*-axis-oriented texture and low surface roughness by annealing at 500 °C. Therefore, it is further used as both piezoelectric layer and substrate for the deposition of FeCoSiB film in the following step.

The optimized conditions of deposition for FeCoSiB film is shown in Table 2. The wafer was first cut into $15 \times 5\ mm^2$ rectangles after depositing FeCoSiB film on $Si/SiO_2/Mo/AlN$ substrates. No bias magnetic field was applied during the deposition of FeCoSiB film. The background pressure before annealing was 5×10^{-4} Pa. The samples were then annealed in a magnetic field of 400 Oe at 250 °C, 300 °C, 350 °C and 400 °C for 40 min with their length parallel to direction of magnetic field. In order to characterize the magnetic properties of the FeCoSiB film, a vibrating sample magnetometer (VSM) was used.

The coercivity variation of FeCoSiB film as a function of annealing temperature is shown in Fig. 7. It should be noted that the first point represents no heat-treatment and therefore the annealing temperature is taken as room temperature (i.e., 25 °C). It can be found that the coercivity H_c decreased by between 40.6% and 54.9% after annealing in magnetic field. Moreover, the H_c decreases firstly and increases afterward with increasing the annealing temperature (the minimum H_c is 2.6 Oe at 350 °C). The decrease of H_c can be attributed to (1) the release of the internal stress, and (2) the improvement of the soft magnetic properties of FeCoSiB film after annealing; while the increase of H_c is owe to that the ordered orientation of atomic magnetic moment was destroyed by thermal disturbance and lead to the loss of uniaxial anisotropy and divergence of magnetic easy axis. Therefore, it can be concluded that the most pronounced magnetic field sensitivity for fields along the parallel orientation could be achieved after annealing at 350 °C. The last but not the least, it should be pointed out that when annealing temperature is above 400 °C, there will be peeling between films and substrate with lots of microcracks shown in three-dimensional (3D) microscopy (Fig. 8). It could be attributed to the excessive internal stress caused by thermal mismatching between films and films or substrates.

Fig. 9 shows the magnetic hysteresis loops of as-deposited FeCoSiB film and annealed at 350 °C measured with fields up to 75 Oe by applying magnetic fields parallel to the film plane (in plane). The saturation magnetizations M_s of as-deposited and annealed loops show 760 emu/cm^3 and 790 emu/cm^3, respectively. In addition, the magnetization of annealed FeCoSiB film has reached saturation at magnetic field of 20 Oe, much lower than that of as-deposited one. This indicated that pronounced magnetic field sensitivity has been produced in FeCoSiB film by means of magnetic field annealing.

3.3. Measurement of ME response

Fig. 10 shows the cross-sectional FESEM image of $Si/SiO_2/Mo/AlN/FeCoSiB$ ME thin film composites, which shows a clear interface boundary between AlN layer with columnar microstructure and FeCoSiB layer with dense microstructure along their growth direction. Such a perfect interface can not be attained in glue-bonded bulk laminates. The AlN layer with (002) preferential orientation has a thickness of ~1.2 μm, while the FeCoSiB layer has a thickness of ~1.5 μm.

The ME measurements were carried out by applying both H_{dc} and small H_{ac} parallel to the film plane (the length direction). The ME voltage coefficient is defined as $\alpha_{ME}=\delta V/d\delta H_{ac}$ (d is the thickness of AlN layer). Fig. 11 shows ME voltage V_{ME} and ME voltage coefficient α_{ME} as a function of H_{dc} measured at $H_{ac}=1$ Oe and $f=1$ kHz. It is well known that the ME response as a function of H_{dc} is consistent with the dependence of effective piezomagnetic coefficient $d_{33,m}$ (i.e., $\delta\lambda/\delta H$, λ is the magnetostriction) on H_{dc} [26,27]. As can be seen from Fig. 11, the magnitude of the ME voltage coefficient α_{ME} starts at some high value (91.42 V/cm Oe) when the magnetic field is 0 Oe. It could be

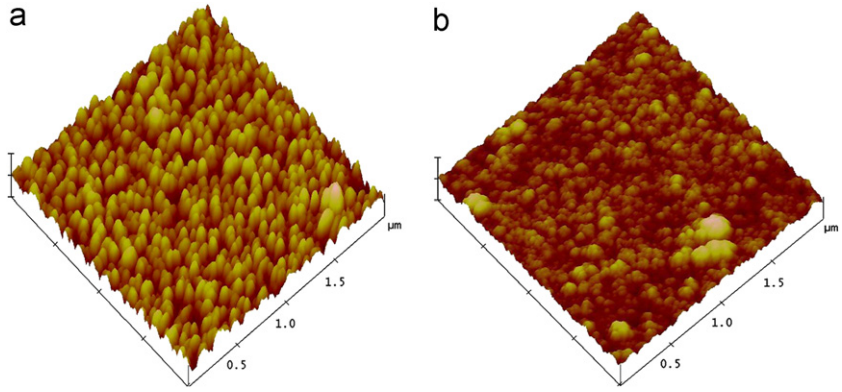

Fig. 6. AFM surface roughness of AlN film deposited on Mo at various annealing temperatures: (a) 3-D view of no annealing, and (b) 3-D view of 500 °C annealing.

Table 2
Deposition parameters for FeCoSiB film.

Target	$(Fe_{90}Co_{10})_{78}Si_{12}B_{10}$ 99.99%
Substrate to target distance (mm)	60
Sputtering gas and pressure (mTorr)	1mTorr Ar
Substrate temperature (°C)	unheated
sputtering time (min)	40
Sputtering power (W)	300

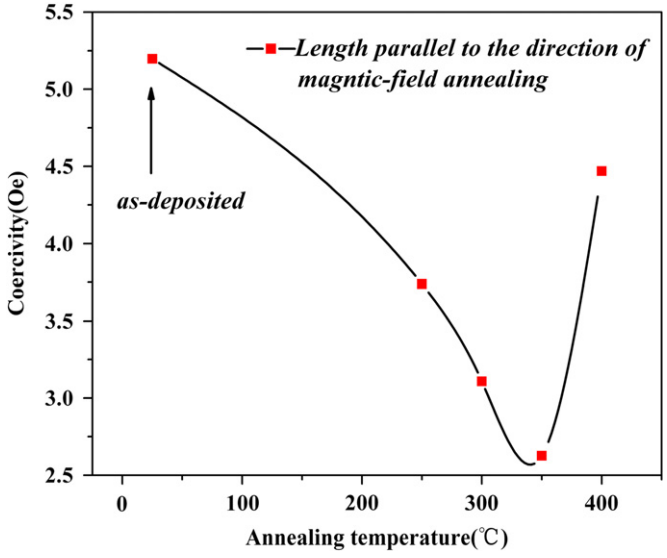

Fig. 7. The coercivity of FeCoSiB film as a function of annealing temperatures.

attributed to (1) the $H_{ac} > 0$ and (2) the high permeability of FeCoSiB film, so that large change in magnetization can be induced in FeCoSiB film by the stress transferred from AlN layer, contributing to the obtaining of large $d_{33,m}$ in FeCoSiB film. With the increase of H_{dc}, the $d_{33,m}$ of FeCoSiB film increases sharply accordingly, giving rise to a rapidly increasing of the value of α_{ME}. As the H_{dc} increases to near 10 Oe, the $d_{33,m}$ is maximized, resulting in a maximum in strain and hence in a maximum in α_{ME} (101 V/cm Oe). It deserves

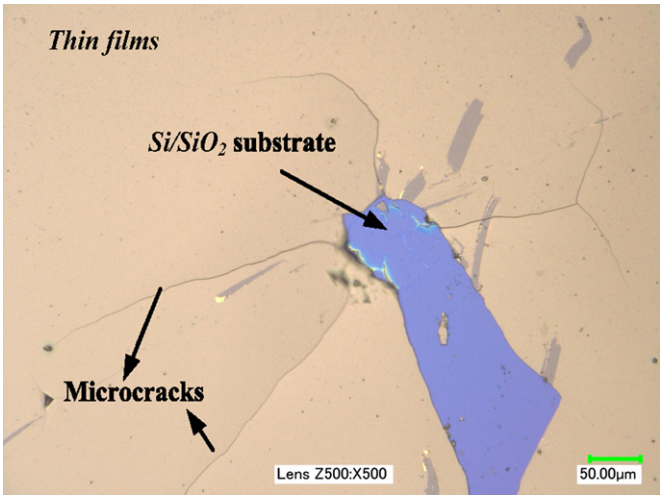

Fig. 8. The surface morphology of AlN/FeCoSiB thin films.

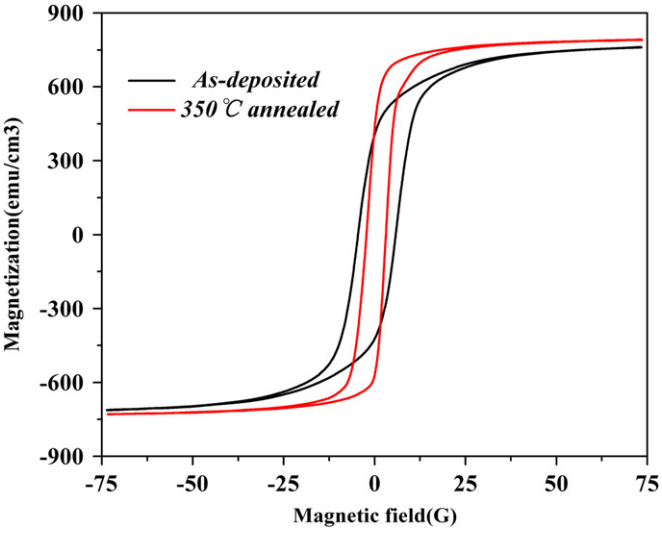

Fig. 9. *M–H* hysteresis loops of as-deposited and 350 °C annealed AlN/FeCoSiB thin film composites by applying magnetic-field parallel to the length of rectangles.

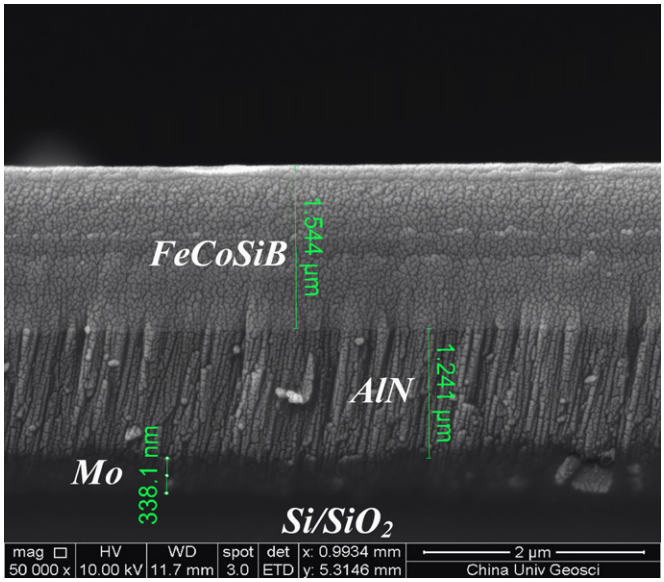

Fig. 10. FESEM cross-sectional of $Si/SiO_2/Mo/AlN/FeCoSiB$ ME thin film composites.

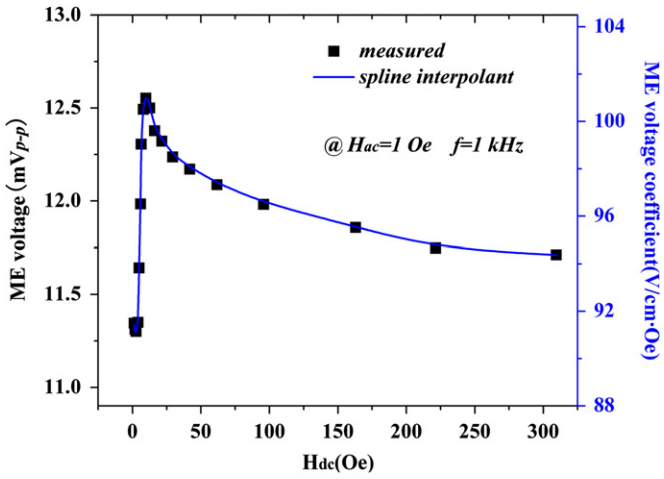

Fig. 11. ME voltage V_{ME} and ME voltage coefficient α_{ME} as a function of DC bias magnetic field H_{dc} at $H_{ac}=1$ Oe and $f=1$ kHz.

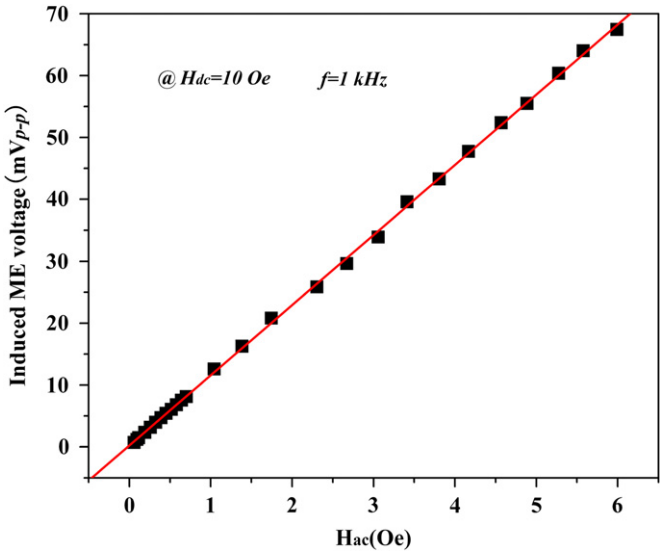

Fig. 12. ME voltage V_{ME} as a function of AC magnetic field H_{ac} at $H_{dc}=10$ Oe and $f=1$ kHz.

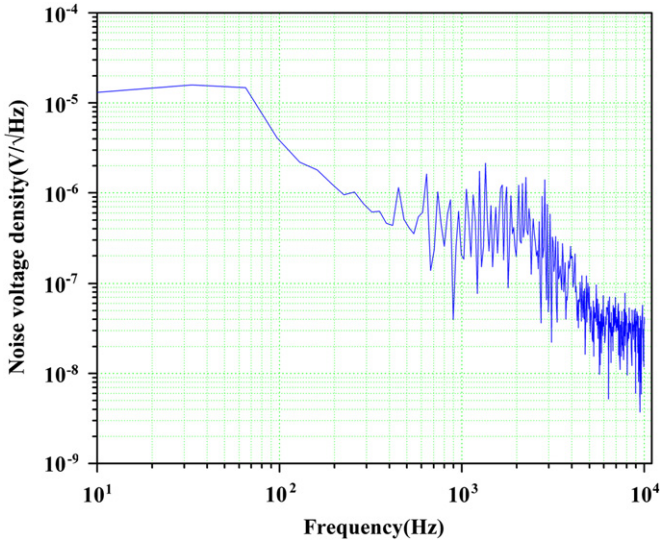

Fig. 13. The measured noise voltage density as a function of frequency.

attention that our thin film composites have an almost linear H_{dc} response in the range of $0 < H_{dc} < 10$ Oe which indicates the possibility to use the AlN/FeCoSiB thin film composites for low-level DC magnetic field detection. With further increase in magnetic field strength, the saturation in magnetostriction of FeCoSiB film gives rise to a decrease in $d_{33,m}$ and strain, and hence a decline in ME response after the rapid increase. In brief, such high ME effect occur due to (1) optimum stress transfer in the L–T configuration, and (2) the large $d_{33,m}$ and high permeability of the FeCoSiB film.

To evaluate the AC magnetic field sensitivity of the current AlN/FeCoSiB ME thin film composites, the induced ME voltage U_{ME} is measured as a function of H_{ac} amplitude under $H_{dc}=10$ Oe and $f=1$ kHz, as shown in Fig. 12. It can be seen that the induced ME voltage V_{ME} was a linear function of H_{ac} in the range of ± 6 Oe, which offers tremendous opportunities to use the AlN/FeCoSiB thin film composites for AC magnetic field detection. From the slope of the V_{ME}–H_{ac} plot, the ME voltage coefficient α_{ME} is calculated to be about 91.4 V/cm Oe using the equation $\alpha_{ME}=\delta V/d\delta H_{ac}$ With an ME voltage coefficient of 91.4 V/cm Oe and the noise voltage at 1 kHz (shown in Fig. 13), one can calculate the AC magnetic field sensitivity of the thin film composites:

$$S = \frac{V_{noise}}{d\alpha_{ME}} = \frac{183.76\,nV/\sqrt{Hz}}{11.34\,mV/Oe} \approx 1.6\frac{nT}{\sqrt{Hz}} \quad (1)$$

4. Conclusions

In summary, the preparation process of AlN/FeCoSiB thin film composites has been studied in detail. The results show

that comparing with changing sputtering parameters, annealing can improve the intensity of AlN (002) peak significantly. After annealing at 500 °C, the AlN film possesses the highest intensity of (002) peak, typical columnar microstructure and rms roughness of 5 nm. The H_c of FeCoSiB film decreased significantly after annealing in magnetic field. The H_c decreases firstly and increases afterward with increasing the annealing temperature. When annealing temperature is above 400 °C, there is peeling between films and substrate, resulting in lots of micro-cracks. The FeCoSiB film annealed at 350 °C has a minimum H_c of 2.6 Oe and M_s of 790 emu/cm^3 at H_{dc} of only 20 Oe.

The Si/SiO_2/Mo/AlN/FeCoSiB ME thin film composites present a clear interface boundary between piezoelectric layer and magnetostrictive layer. The ME voltage coefficient α_{ME} increases to the maximum 101 V/cm Oe at H_{dc} of only 10 Oe and then decreases with increasing H_{dc}. In addition, the induced ME voltage is a linear function of H_{ac} in the range of ± 6 Oe, measured at $H_{dc}=10$ Oe and $f=1$ kHz. Further more, the thin film composites display an AC magnetic field sensitivity of 1.6 nT/$\sqrt{}$Hz at 1 kHz. The AlN/FeCoSiB thin film composites prepared in this work shows great potential in application of magnetic detection in the view of ME properties above.

Acknowledgments

This project is based on work supported by the National Natural Science Foundation Program of China (No. 51172080).

References

[1] K.F. Wang, J.M. Liu, Z.F. Ren, Multiferroicity: the coupling between magnetic and polarization orders, Advances in Physics 58 (2009) 321–448.
[2] N.A. Spaldin, M. Fiebig, The renaissance of magnetoelectric multiferroics, Science 309 (2005) 391–392.
[3] C.W. Nan, M.I. Bichurin, S.X. Dong, D. Viehland, G. Srinivasan, Multiferroic magnetoelectric composites: historical perspective, status, and future directions, Journal of Applied Physics 103 (2008) 031101–031135.
[4] S.X. Dong, J.Y. Zhai, J.F. Li, D. Viehland, Magnetoelectric effect in Terfenol-D/Pb (Zr, Ti) O_3/μ-metal laminate composites, Applied Physics Letters 89 (2006) 122903–122905.
[5] J.P. Zhou, H.C. He, Z. Shi, C.W. Nan, Magnetoelectric $CoFe_2O_4$/Pb ($Zr_{0.52}$ $Ti_{0.48}$) O_3 double-layer thin film prepared by pulsed-laser deposition, Applied Physics Letters 88 (2006) 013111–013113.
[6] E. Lage, C. Kirchhof, V. Hrkac, L. Kienle, R. Jahns, R. Knochel, E. Quandt, D. Meyners, Exchange biasing of magnetoelectric composites, Nature Materials 11 (2012) 523–529.
[7] J. Ma, J.M. Hu, Z. Li, C.W. Nan, Recent progress in multiferroic magnetoelectric composites: from bulk to thin films, Advanced Materials 23 (2011) 1062–1087.
[8] N. Tiercelin, A. Talbi, V. Preobrazhensky, P. Pernod, V. Mortet, K. Haenen, A. Soltani, Magnetoelectric effect near spin reorientation transition in giant magnetostrictive-aluminum nitride thin film structure, Applied Physics Letters 93 (2008) 162902–162904.
[9] M. Bibes, A. Barthelemy, Multiferroics: towards a magnetoelectric memory, Nature Materials 7 (2008) 425–426.
[10] Y. Zhang, Z. Li, C.Y. Deng, J. Ma, Y.H. Lin, C.W. Nan, Demonstration of magnetoelectric read head of multiferroic heterostructures, Applied Physics Letters 92 (2008) 152510–152512.
[11] I. Levin, J.H. Li, J. Slutsker, A.L. Roytburd, Design of self-assembled multiferroic nanostructures in epitaxial films, Advanced Materials 18 (2006) 2044–2047.
[12] J.P. Zhou, Z.C. Qiu, P. Liu, Electric and magnetic properties of Pb ($Zr_{0.52}Ti_{0.48}$) O_3–$CoFe_2O_4$ particle composite thin film on the $SrTiO_3$ substrate, Materials Research Bulletin 43 (2008) 3514–3520.
[13] J.P. Zhou, H.C. He, Y. Zhang, C.Y. Deng, Z. Shi, C.W. Nan, Electric and magnetic properties of $CoFe_2O_4$/Pb ($Zr_{0.52}Ti_{0.48}$) O_3bilayer thin films prepared by pulsed-laser deposition, Applied Physics A-Materials Science and Processing 89 (2007) 553–558.
[14] C.Y. Deng, Y. Zhang, J. Ma, Y.H. Lin, C.W. Nan, Magnetoelectric effect in multiferroic heteroepitaxial $BaTiO_3$–$NiFe_2O_4$ composite thin films, Acta Materialia 56 (2008) 405–412.
[15] J.X. Zhang, J.Y. Dai, C.K. Chow, C.L. Sun, V.C. Lo, H.L.W. Chan, Magnetoelectric coupling in $CoFe_2O_4$/$SrRuO_3$/Pb ($Zr_{0.52}Ti_{0.48}$) O_3 heteroepitaxial thin film structure, Applied Physics Letters 92 (2008) 022901–022903.
[16] J.G. Wan, X.W. Wang, Y.J. Wu, M. Zeng, Y. Wang, H. Jiang, W.Q. Zhou, G.H. Wang, J.M. Liu, Magnetoelectric $CoFe_2O_4$–Pb (Zr, Ti) O_3 composite thin films derived by a sol–gel process, Applied Physics Letters 86 (2005) 122501–122503.
[17] P. Zhao, Z.L. Zhao, D. Hunter, R. Suchoski, C. Gao, S. Mathews, M. Wuttig, I. Takeuchi, Fabrication and characterization of all-thin-film magnetoelectric sensors, Applied Physics Letters 94 (2009) 243507–243509.
[18] M. Feng, W. Wang, J.C. Rao, Y. Zhou, D.C. Jia, H.B. Li, Microstructural, electrical and magnetic properties of multiferroic $CoFe_2O_4$/0.68Pb ($Mg_{1/3}Nb_{2/3}$)O_3–0.32$PbTiO_3$ nanocomposite thin films, Ceramics International 37 (2011) 3045–3048.
[19] Z. Li, Y. Gao, B. Yang, Y.H. Lin, R. Yu, C.W. Nan, Influence of stress and orientation on magnetoelectric coupling of Pb (Zr, Ti) O_3–$CoFe_2O_4$ bilayer films, Journal of American Ceramic Society 94 (2011) 1060–1066.
[20] H. Greve, E. Woltermann, H.J. Quenzer, B. Wagner, E. Quandt, Giant magnetoelectric coefficients in $(Fe_{90}Co_{10})_{78}Si_{12}B_{10}$–AlN thin film composites, Applied Physics Letters 96 (2010) 182501–182503.
[21] H. Greve, E. Woltermann, R. Jahns, S. Marauska, B. Wagner, R. Knochel, M. Wuttig, E. Quandt, Low damping resonant magnetoelectric sensors, Applied Physics Letters 97 (2010) 152503–152505.
[22] R. Jahns, H. Greve, E. Woltermann, E. Quandt, R.H. Knochel, Noise performance of magnetometers with resonant thin-film magnetoelectric sensors, IEEE Transactions on Instrumentation and Measurement 60 (2011) 2995–3001.
[23] C.L. Huang, K.W. Tay, L. Wu, Aluminum nitride films deposited under various sputtering parameters on molybdenum electrodes, Solid-State Electronics 49 (2005) 219–225.
[24] H. Jin, J. Zhou, S.R. Dong, B. Feng, J.K. Luo, D.M. Wang, W.I. Milne, C.Y. Yang, Deposition of *c*-axis orientation aluminum nitride films on flexible polymer substrates by reactive direct-current magnetron sputtering, Thin Solid Films 520 (2012) 4863–4870.
[25] J.S. Cherng, T.Y. Chen, Influence of sputtering atmosphere on polarity distribution of piezoelectric aluminum nitride thin films, Current Applied Physics 11 (2011) S371–S375.
[26] S.X. Dong, J.Y. Zhai, F.M. Bai, J.F. Li, D. Viehland, Push-pull mode magnetostrictive/piezoelectric laminate composite with an enhanced magnetoelectric voltage coefficient, Applied Physics Letters 87 (2005) 062502–062504.
[27] J.L. Hockel, T. Wu, G.P. Carman, Voltage bias influence on the converse magnetoelectric effect of PZT/Terfenol-D/PZT laminates, Journal of Applied Physics 109 (2011) 064106.